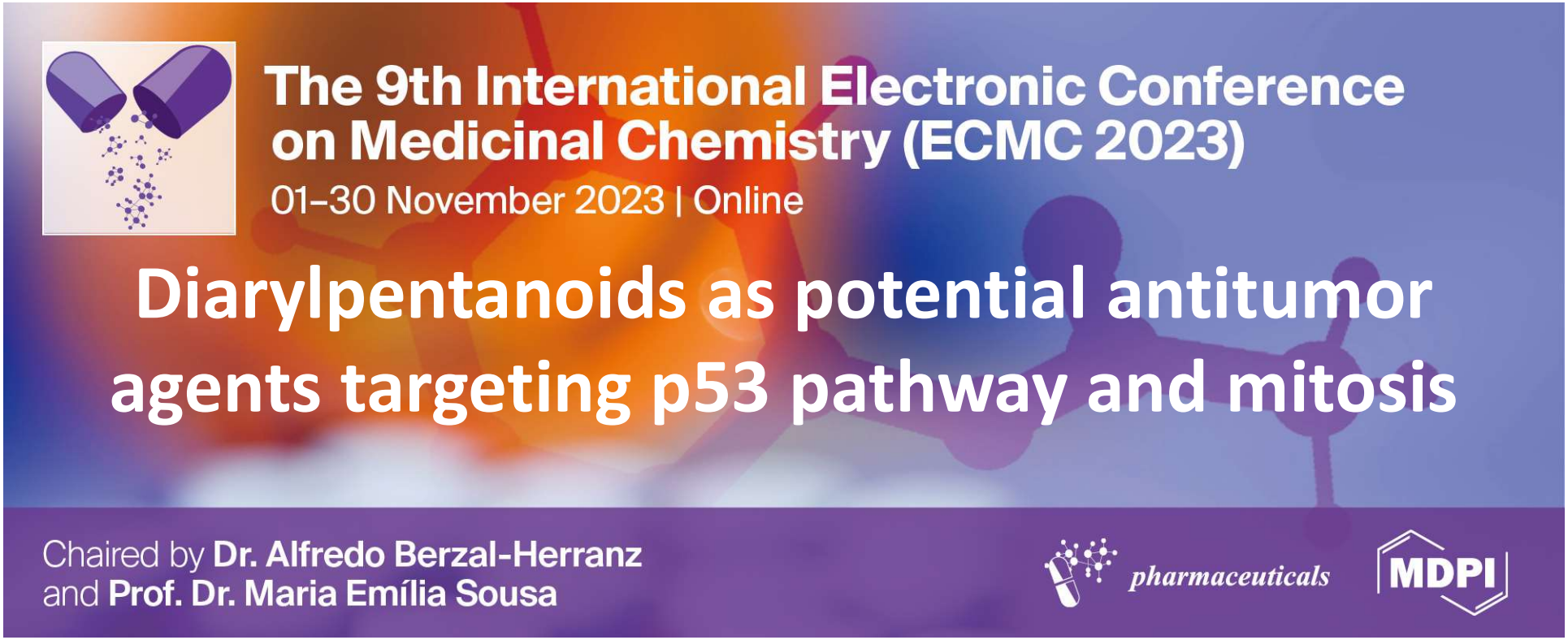

Honorina Cidade*

[1] Laboratory of Organic and Pharmaceutical Chemistry, Department of Chemical Sciences, Faculty of Pharmacy of University of Porto, Rua de Jorge Viterbo Ferreira 228, 4050-313 Porto, Portugal

[2] Interdisciplinary Centre of Marine and Environmental Research (CIIMAR), University of Porto, Edifício do Terminal de Cruzeiros do Porto de Leixões, Avenida General Norton de Matos, S/N, 4450-208 Matosinhos, Portugal

* Corresponding author: hcidade@ff.up.pt

The 9th International Electronic Conference on Medicinal Chemistry
01–30 November 2023 | Online

Diarylpentanoids as potential antitumor agents targeting p53 pathway and mitosis

Graphical Abstract

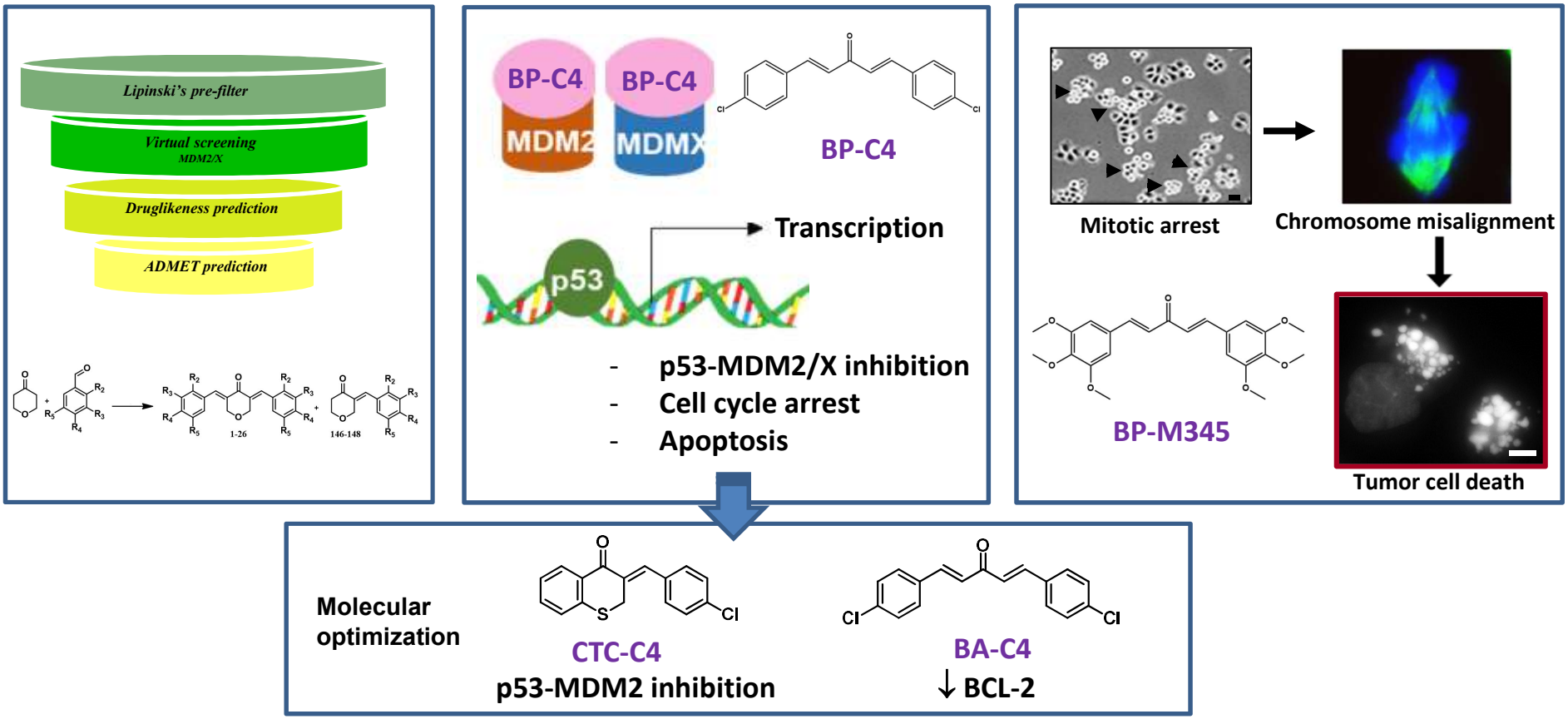

Abstract:

Diarylpentanoids are chalcone analogues with two aromatic rings connected by a five-carbon bridge, showing a wide range of biological activities, being the *in vitro* growth inhibitory activity against cancer cells one of the most studied. However, the underlying mechanisms by which these compounds suppress cancer cell growth is still unclear. Our research group has reported several chalcones with notable antiproliferative activity in human cancer cells. Particularly, chalcone **CM-M345** showed potent growth inhibitory activity against a panel of cancer cells, being this associated with the interference with the interaction between the tumor suppressor protein p53 and its endogenous negative regulator MDM2. In this communication, the design, synthesis, and biological evaluation of analogues of **CM-M345** with diarylpentanoid scaffold showing promising antitumor activity are explored. From these studies new diarylpentanoids with promising antitumor effect through the interference with p53 pathway and mitosis have emerged. Our results show, for the first time, that exploration of diarylpentanoid scaffold can result in the discovery of new potential p53-MDM2/X dual inhibitors as well as promising antimitotic agents, which may be used as starting point for the discovery of new drug candidates for cancer therapy.

Keywords: cancer; chalcones; diarylpentanoids; MDM2; MDMX; mitosis; p53

Introduction

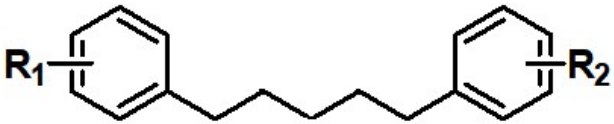

Diarylpentanoids

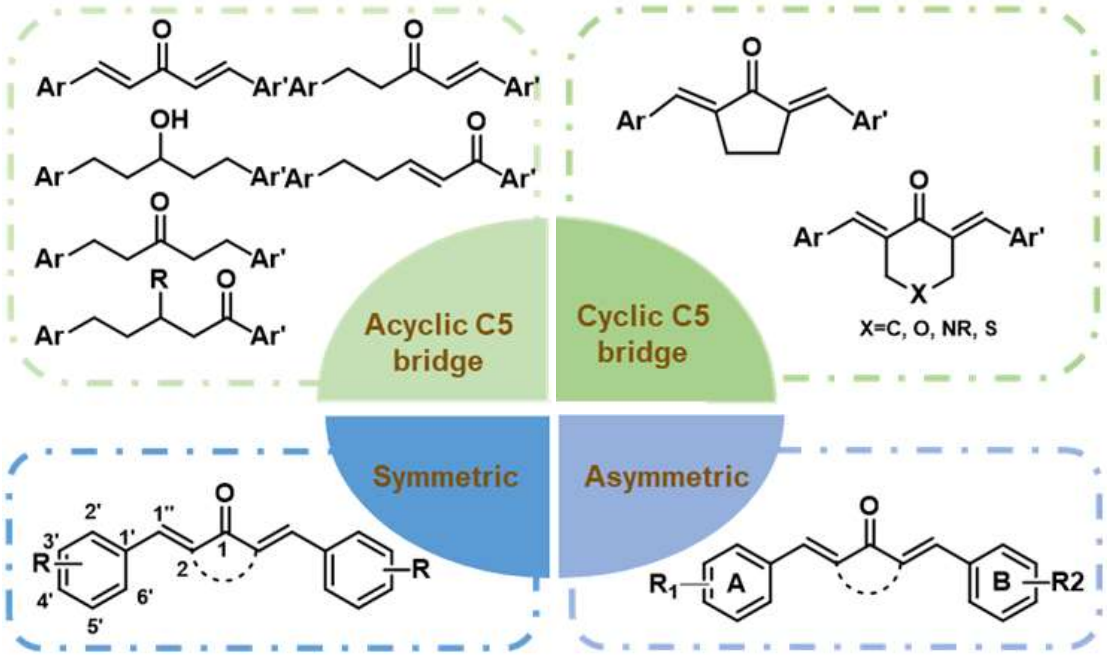

Structure related with chalcones

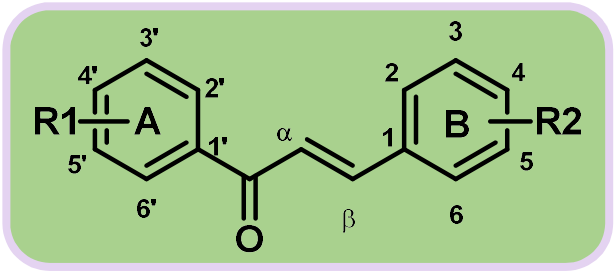

Moreira J. *et al.*, *Eur J Med Chem*, 2020, 192,112177, https://doi.org/10.1016/j.ejmech.2020.112177.

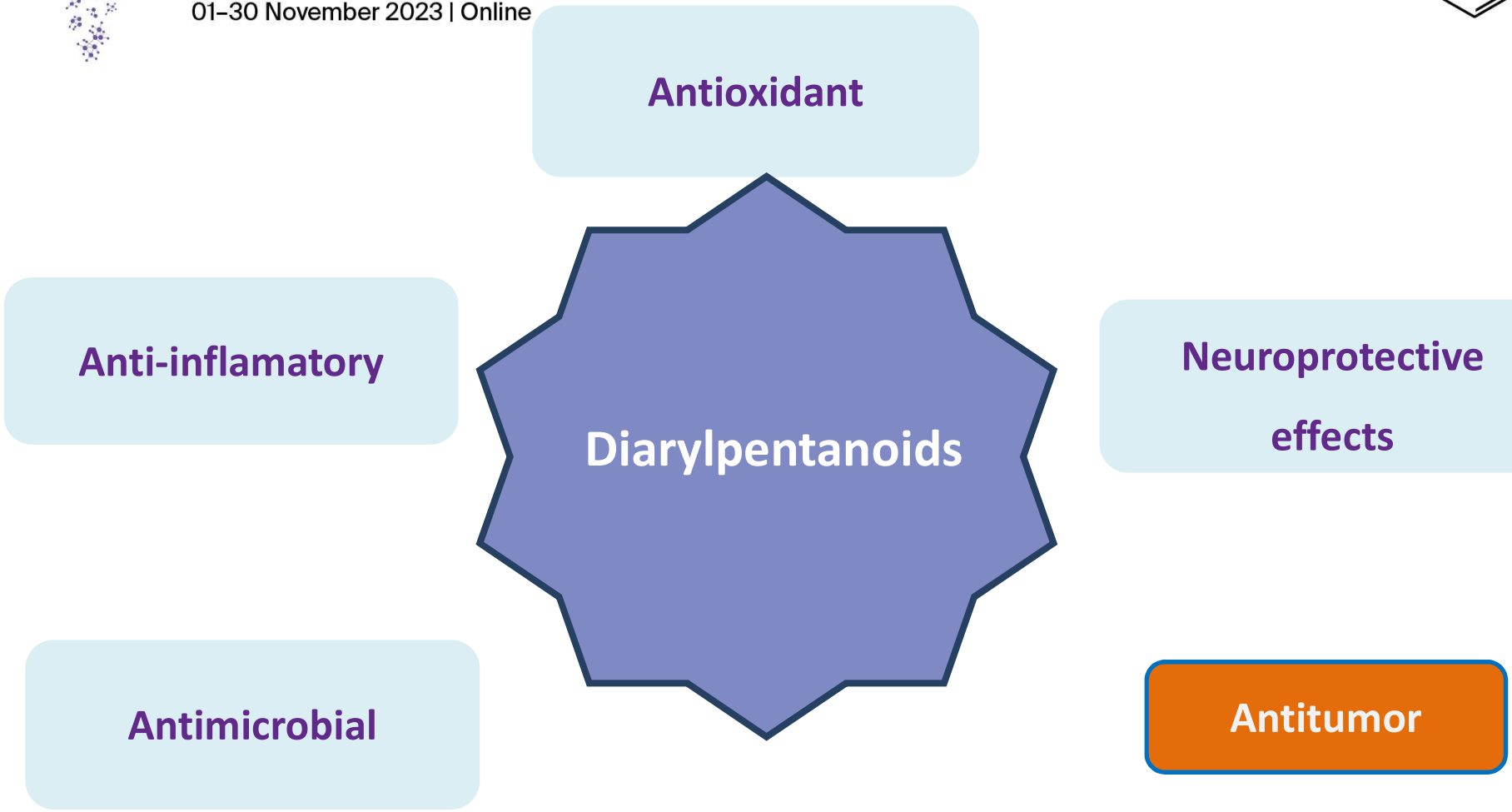

- ✓ **Molecular mechanism by which these compounds suppress cancer cell growth is still unclear**
- ✓ **The interference with p53 pathway was suggested**

Moreira J. *et al*., *Eur J Med Chem*, 2020, 192,112177, https://doi.org/10.1016/j.ejmech.2020.112177; Moreira J. *et al*., *Molecules*, 2022, 27, 6340, https://doi.org/10.3390/molecules27196340

Why p53?

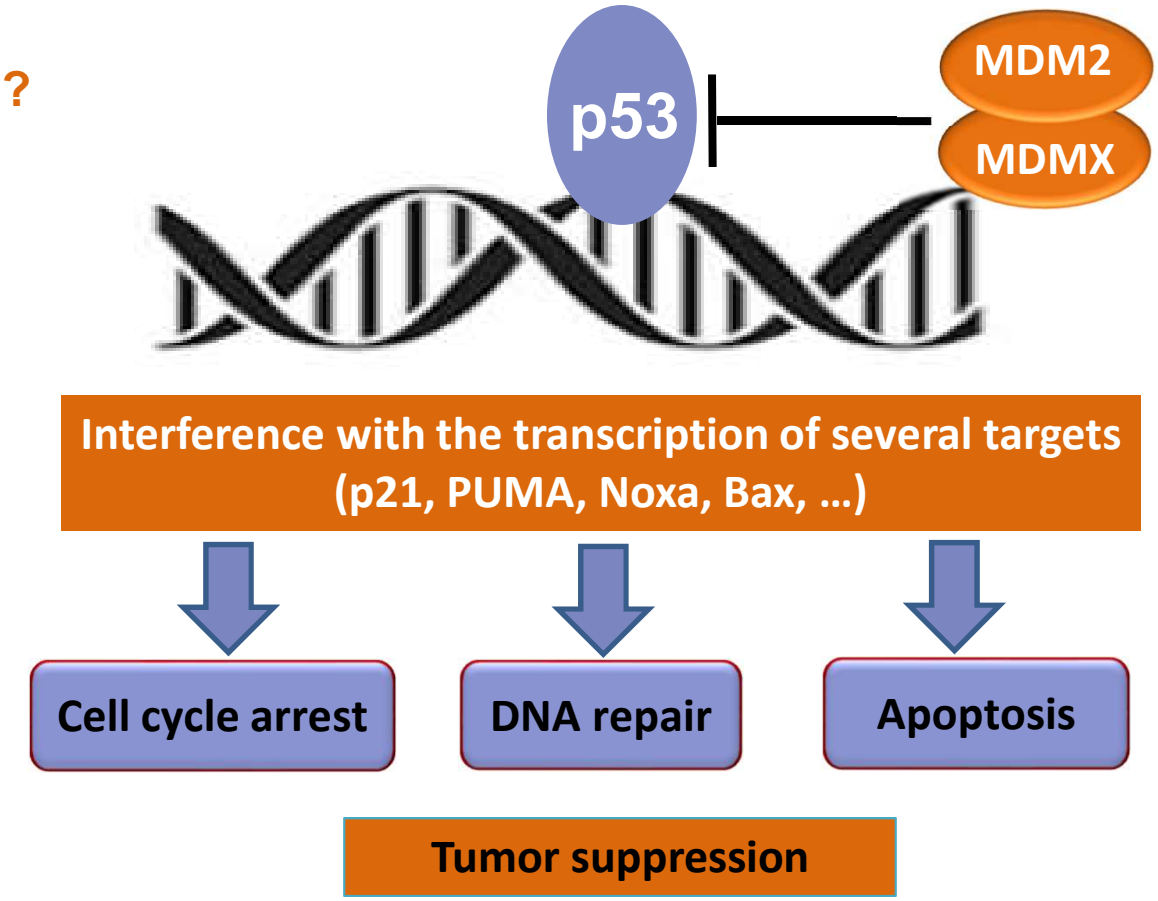

All types of cancers have inactivated p53, either by mutation of TP53 gene or inhibition due to the overexpression of the endogenous negative regulators MDM2/X

Lemos A. *et al*., *Med Res Rev*. 2016; 36(5):789-844.

Research plan

Chalcones with antitumor activity as inhibitors of p53-MDM2 interaction

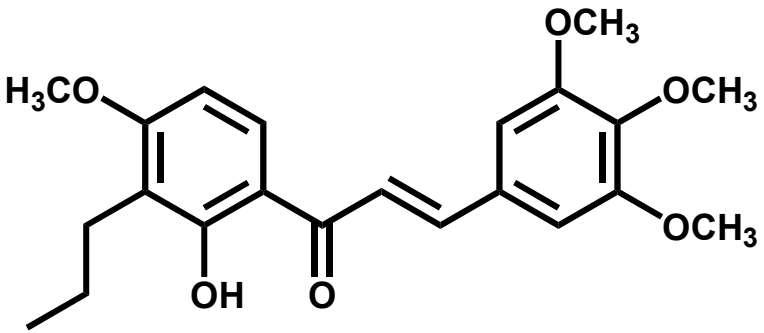

CM-M345

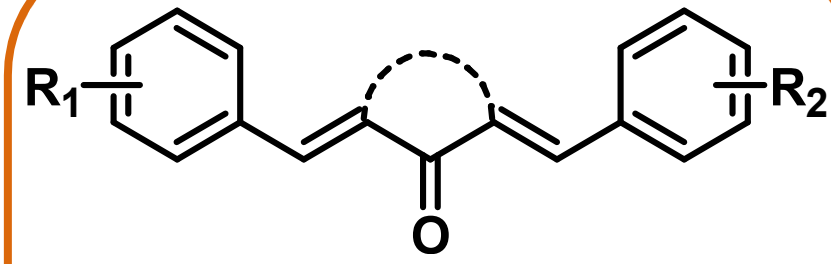

…have shown *in vitro* growth inhibitory effect on tumor cells associated with an increase of p53 expression;

… the interference of these compounds with p53-MDM2/X interactions was never explored.

Aim

To obtain new diarylpentanoids with antitumor activity by inhibiting the p53-MDM2/X interactions

Pereira D. *et al.*, *Arabian J. Chem.,* 2019, 12, 4150-4161; Moreira J. *et al.*, *Eur J Med Chem*, 2020, 192,112177, https://doi.org/10.1016/j.ejmech.2020.112177.

Results and Discussion

In silico studies

VIRTUAL SCREENING

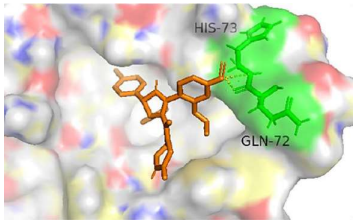

Target: MDM2
Positive control: Nutlin 3A
AutoDock Vina

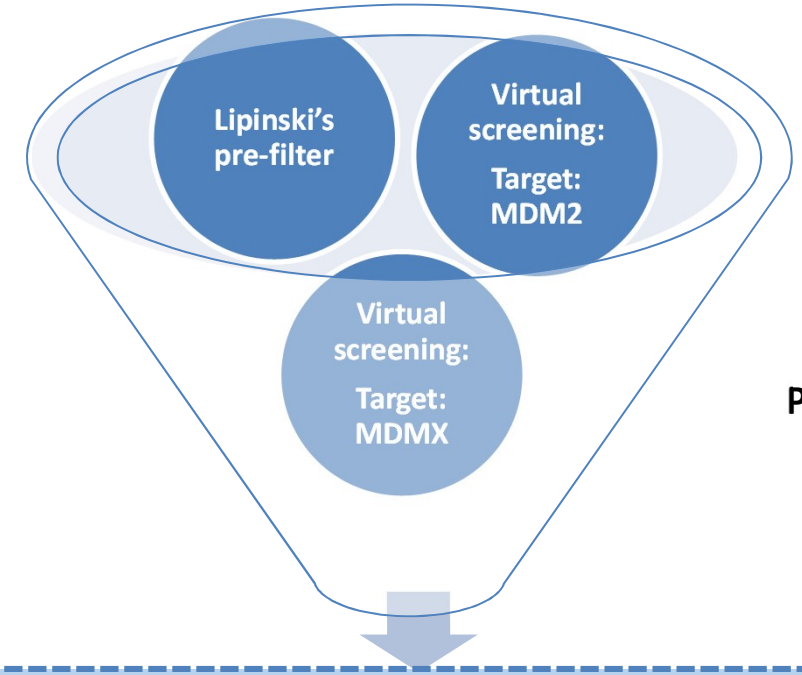

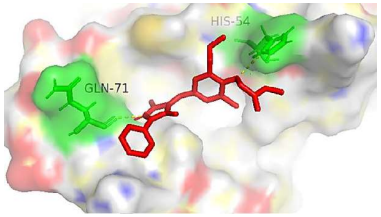

Target: MDMX
Positive control: SJ-172550
AutoDock Vina

For diarylpentanoids with the best docking scores:

Druglikeness Prediction (SwissADME* web server; PreADMET** web server)

ADMET prediction (PreADMET web server)

*http://www.swissadme.ch/

**https://preadmet.bmdrc.kr/

Moreira J. *et al.*, *ChemMedChem*, 2021, 16 (19), 2969-2981.

Synthesis

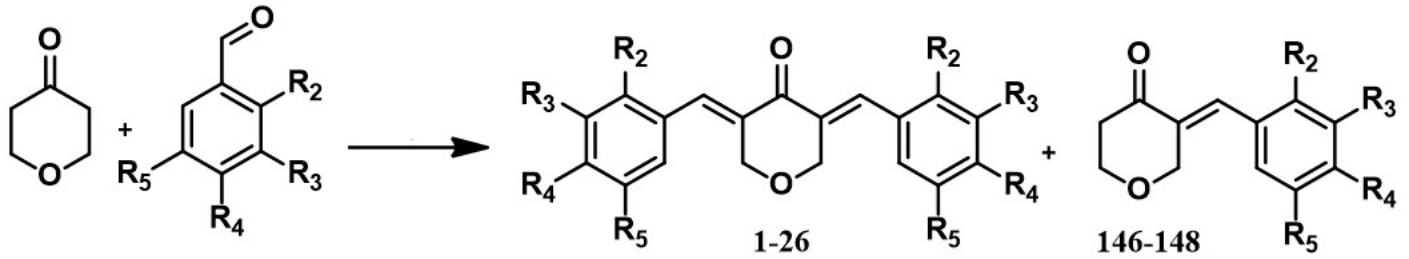

1-13, **17-26**: η=56-87%

14-16, **146-148**: η=20-42%

Compound ID	R_2	R_3	R_4	R_5
1	Br	H	H	H
2	Cl	H	H	H
3	F	H	H	H
4	OCH_3	H	H	H
5	CH_3	H	H	H
6	H	Br	H	H
7	H	OCH_3	H	H
8	H	CH_3	H	H
9	H	H	Br	H
10	H	H	Cl	H
11	H	H	F	H
12	H	H	OCH_3	H
13	H	H	CH_3	H
14, 146	H	H	$N(CH_3)_2$	H

Compound ID	R_2	R_3	R_4	R_5
15, 147	H	H	$N(CH_2CH_3)_2$	H
16, 148	H	H	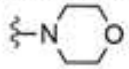	H
17	$-OCH_2O-$		H	H
18	OCH_3	OCH_3	H	H
19	OCH_3	H	OCH_3	H
20	OCH_3	H	H	OCH_3
21	H		$-OCH_2O-$	H
22	H	OCH_3	OCH_3	H
23	H	OCH_3	H	OCH_3
24	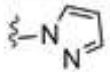	H	H	F
25	OCH_3	H	OCH_3	OCH_3
26	H	OCH_3	OCH_3	OCH_3

Moreira J. *et al*., *ChemMedChem*, 2021, 16 (19), 2969-2981.

MDPI

Collaboration with

LAQV REQUIMTE
Lucília Saraiva

Effect of compounds on the *in vitro* growth of human cell lines

Compound ID	GI_{50} (μM) HCT116 $p53^{+/+}$	GI_{50} (μM) HFF-1	SI*
1,2,12-16,25,146-148	> 25	-----	-----
3	0.69 ± 0.21	0.77 ± 0.30	1.12
4	2.45 ± 0.07	1.44 ± 0.12	0.59
5	3.8 ± 0.42	3.24 ± 0.01	0.85
6	0.9 ± 0.14	0.63 ± 0.008	0.7
7	0.99 ± 0.01	0.55 ± 0.15	0.56
8	1.21 ± 0.01	3.88 ± 0.022	3.21
9	10.1 ± 4.85	9.45 ± 2.62	0.94
10	**6.25 ± 1.18**	**36.20 ± 5.54**	**5.79**
11	0.71 ± 0.08	0.55 ± 0.01	0.77
17	0.64 ± 0.03	0.59 ± 0.005	0.92
18	0.68 ± 0.02	0.89 ± 0.07	1.31
19	1.65 ± 0.64	2.21 ± 0.08	1.34
20	0.87 ± 0.03	0.63 ± 0.03	0.72
21	4.55 ± 0.95	14.76 ± 2.21	3.24
22	1.75 ± 0.10	0.69 ± 0.04	0.39
23	0.63 ± 0.01	0.49 ± 0.01	0.78
24	0.22 ± 0.02	0.33 ± 0.06	1.5
26	**0.17 ± 0.01**	**1.21 ± 0.07**	**7.12**

The results are expressed as mean ± standard deviation from three independent experiments.*SI: selective index (GI_{50} of HFF-1/GI_{50} of HCT116 $p53^{+/+}$); HCT116 $p53^{+/+}$: human colorectal tumor cell; HFF-1: fibroblasts, non-tumor cell line.

Compounds BP-C4 (10) and BP-M345 (26) showed potent and seletive growth inhibitory effect on HCT116 cells

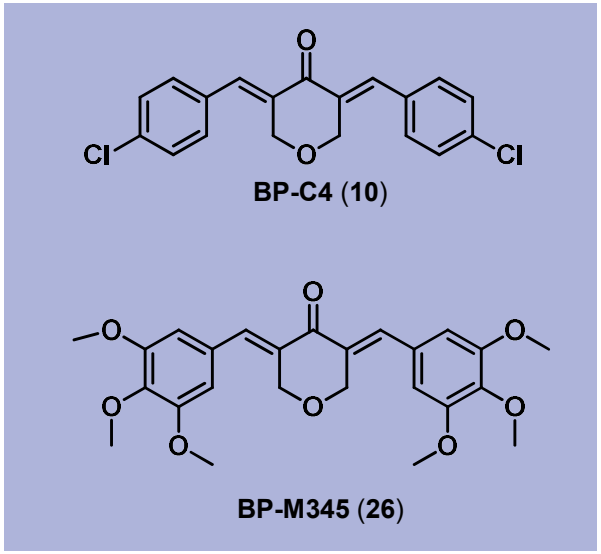

Moreira J. *et al.*, *ChemMedChem*, 2021, 16 (19), 2969-298.

Study of the mechanism of action of BP-C4 (10) and BP-M345 (26)

✓ **BP-C4 (10) showed to be potential inhibitor of the p53-MDM2 (A) and p53-MDMX (B) interactions using yeast-based assay**

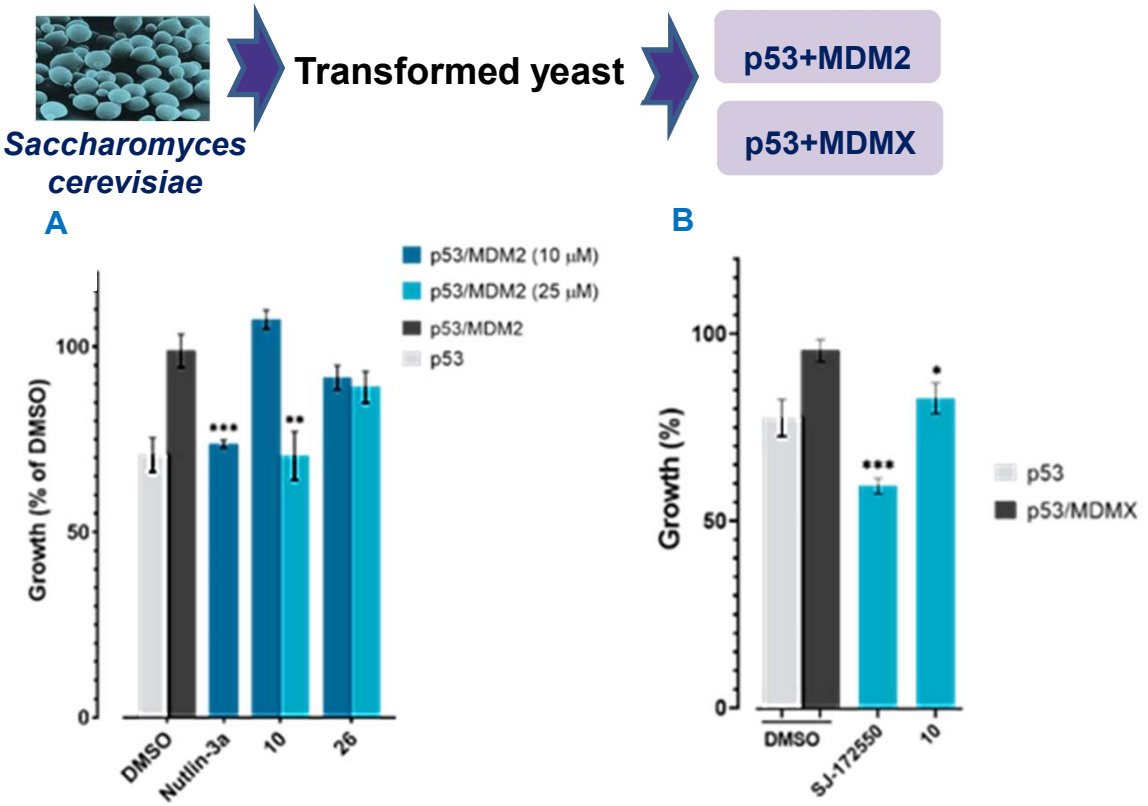

Data are mean ± SEM of at least five independent experiments; values significantly different from DMSO are indicated (***p<0.001, **p<0.01, *p<0.05). The unpaired student t-test was used.

Reversion of the MDM2/X inhibitory effect on p53-induced yeast growth inhibition

Moreira J. *et al.*, *ChemMedChem*, 2021, 16 (19), 2969-298.

In the absence of p53, the inhibitory effect of BP-C4 was significantly reduced

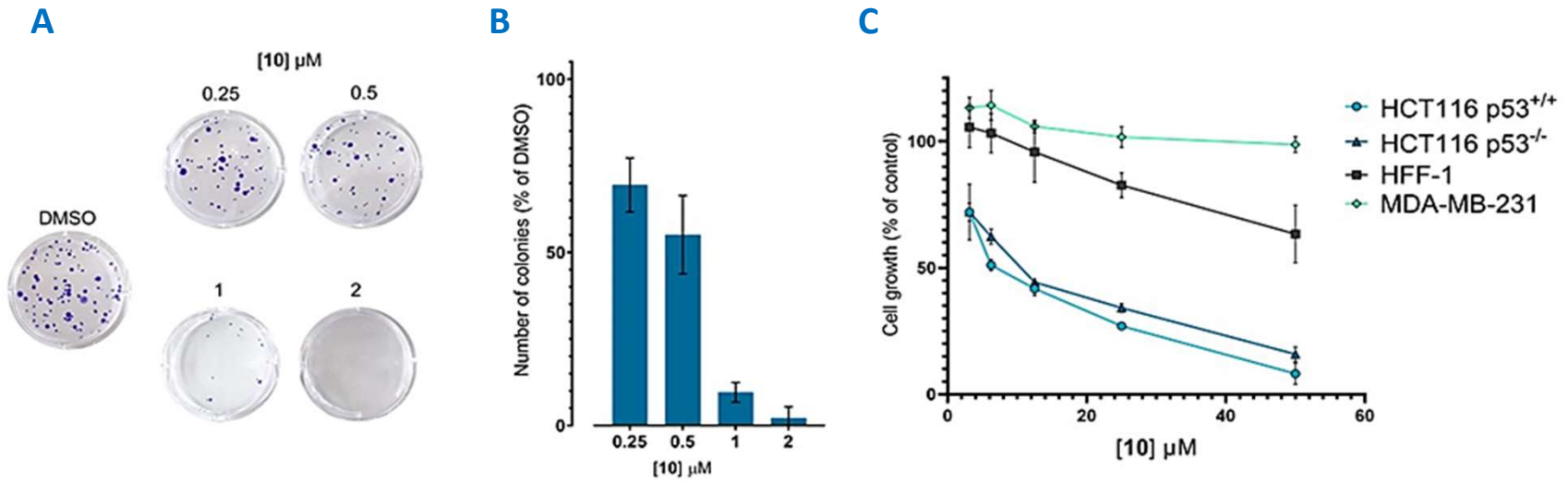

A, **B**: Effect of **BP-C4** (**10**) on the colony formation of HCT116 $p53^{+/+}$ cells. Cells were treated with **BP-C4** (**10**) or solvent for 24 h, and colonies were allowed to grow for 11 days. **A:** Images correspond to a representative experiment of three. **B:** The DMSO-treated cells were considered as 100% growth; data are mean ± SEM of three independent experiments. **C:** Dose-response curves for the growth inhibitory activity of **BP-C4** (**10**) in $p53^{+/+}$ and $p53^{-/-}$ HCT116 cells, HFF-1 and MDA-MB-231 cells, determined by SRB assay, after 48 h treatment. Data are mean ± SEM of three independent experiments.

✓ **BP-C4 induced apoptotic cell death (A) and cell cycle arrest at G0/G1 phase (B), increased the p53 expression levels, p21 and the pro-apoptotic protein PUMA and induced PARP cleavage (C)**

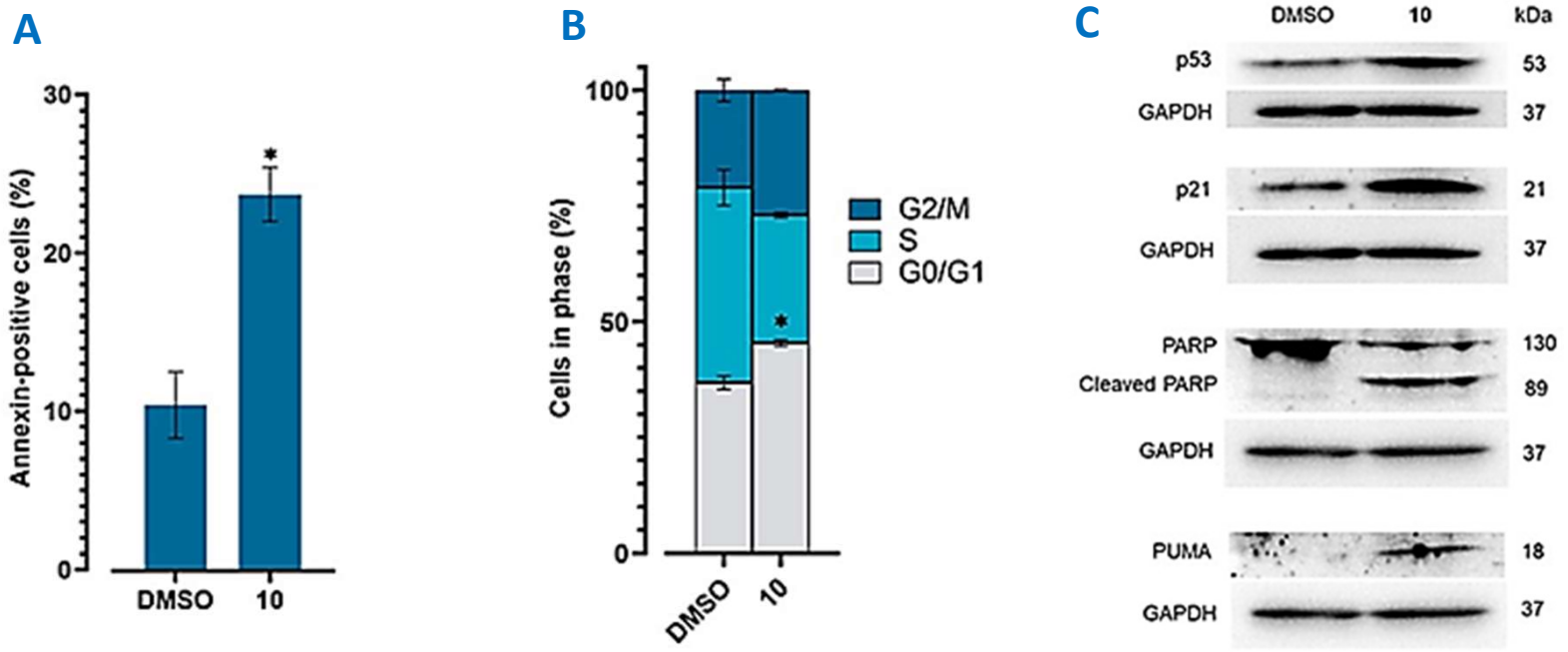

Data are mean ± SEM of three independent experiments; values significantly different from DMSO: *p<0.05. The unpaired student t-test was used. Immunoblots represent two independent experiments; GAPDH was used as a loading control.

BP-C4: potent antitumor activity associated with the activation of the p53 pathway

Moreira J. *et al.*, *ChemMedChem*, 2021, 16 (19), 2969-298.

Identified as promising antiproliferative agents with selectivity for tumor cells

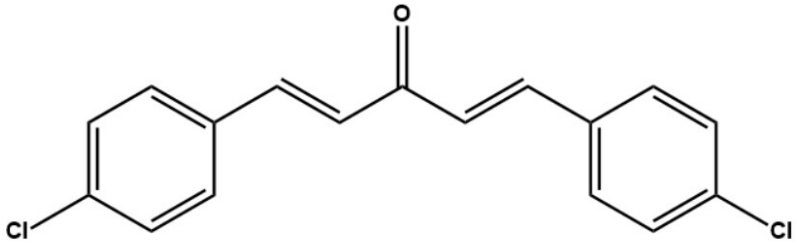

BP-C4
Dual Inhibitor of p53-MDM2/X interactions

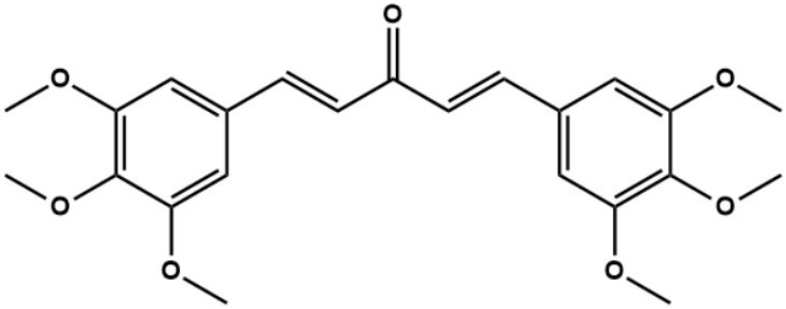

BP-M345

Mechanism?

Microtubule-targeting agents with a 3,4,5-trimethoxyphenyl group

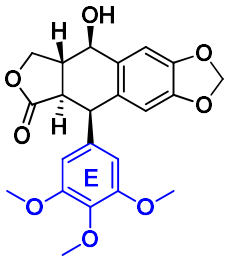

Podophyllotoxin

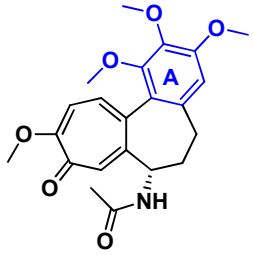

Colchicine

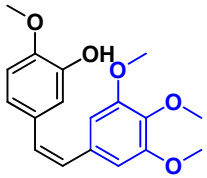

Combretastatin A4

Contents lists available at ScienceDirect
European Journal of Medicinal Chemistry
journal homepage: http://www.elsevier.com/locate/ejmech
ELSEVIER

Research paper

Chalcone derivatives targeting mitosis: synthesis, evaluation of antitumor activity and lipophilicity

Patricia Pinto [a, 1], Carmen Mariana Machado [b, 1], Joana Moreira [b, c, 1], José Diogo P. Almeida [d], Patrícia M.A. Silva [d], Ana C. Henriques [d], José X. Soares [e], Jorge A.R. Salvador [a, f], Carlos Afonso [b, c], Madalena Pinto [b, c], Hassan Bousbaa [d, **], Honorina Cidade [b, c, *]

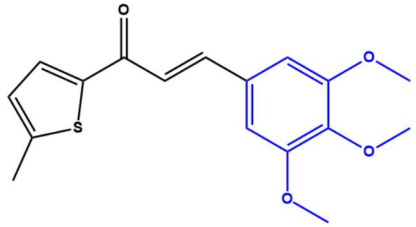

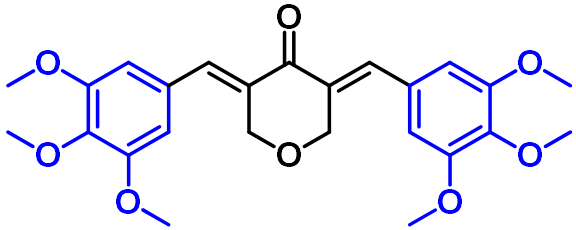

BP-M345

Could this diarylpentanoid also act as an antimitotic agent?

Negy A. S. *et al.*, *Bioorganic & Med Chem*, 2015, 23 (3), 373-89; Fonseca J. *et al.*, *Molecules* 2016, 21(8), 982-996; K. Masawang *et. al.*, *Toxicol. Lett.* 2014, 229, 393-401.

molecules
MDPI

Collaboration with

Hassan Bousbaa

Article

BP-M345, a New Diarylpentanoid with Promising Antimitotic Activity

Pedro Novais [1,2,3,†], Patrícia M. A. Silva [1,4,†], Joana Moreira [5,6], Andreia Palmeira [5,6], Isabel Amorim [7], Madalena Pinto [5,6], Honorina Cidade [5,6,*] and Hassan Bousbaa [1,*]

A.

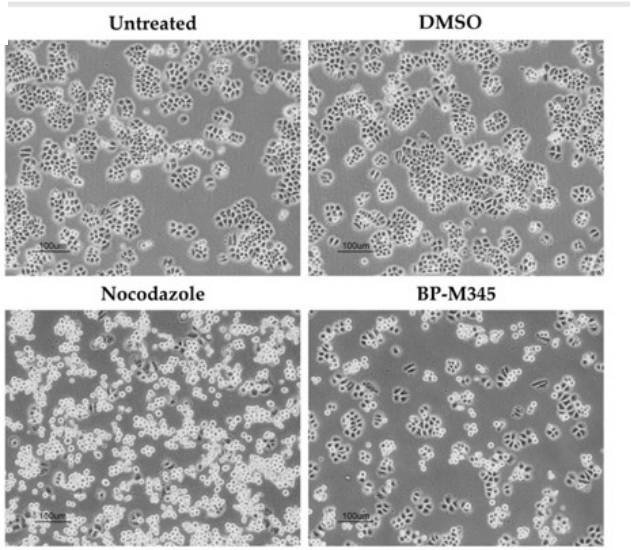

B.

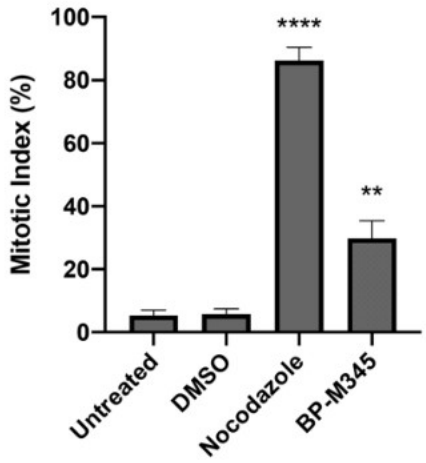

(A) Representative phase contrast microscopy images of untreated cells and cells treated with 0.74 µM of BP-M345, for 16 hours. Cells treated with DMSO and nocodazole were used as controls. Bar, 100 µm. **(B)** Mitotic index of data shown in A with statistical relevance of ** $p < 0.01$ and **** $p < 0.0001$ by unpaired t-test from three independent experiments.

Treatment with BP-M345 arrests NCI-H460 cells in mitosis (MI = 29.8 ± 5.6%)

Novais P. *et al., Molecules*, 2021, 26, 7139. https://doi.org/10.3390/molecules26237139.

BP-M345 treatment disturbs mitotic spindle morphology.
Immunofluorescence images of untreated cells and cells treated with 0.74 µM of BP-M345. Microtubules (green) were stained with anti-α-tubulin antibody and DNA (blue) with DAPI. Bar, 5 µm.

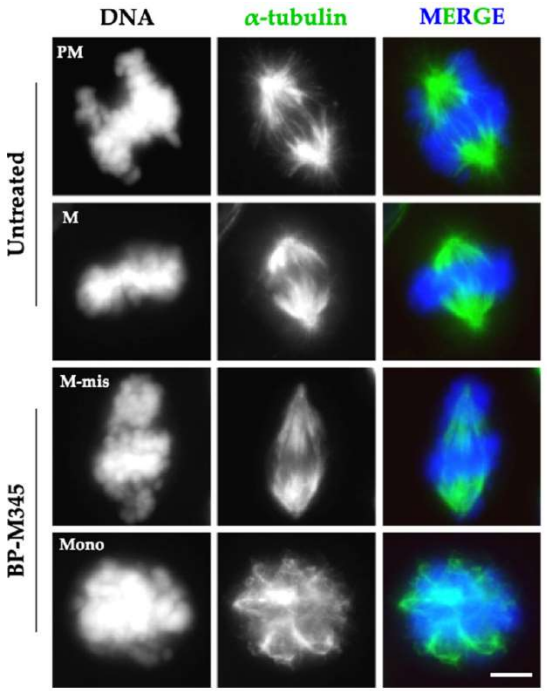

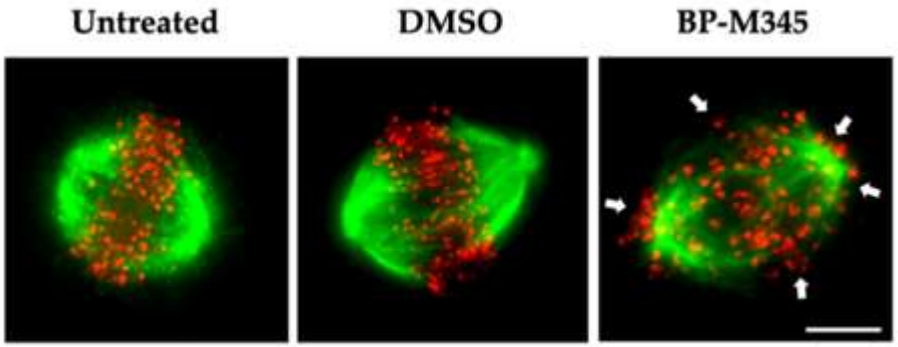

Treatment with BP-M345 interferes with the stability of kinetochore-microtubule attachments.
Representative immunofluorescence images after cold treatment assay, showing several unattached kinetochores (free red spots pointed by the white arrowheads) in cells treated with 0.74 µM of BP-M345 treatment, whereas most kinetochores were attached (Red spots with attached green fibers) in untreated cells. Microtubules (green) were stained with anti-α-tubulin antibody, and kinetochores (red) with anti-CREST antibody.

Novais P. *et al.*, *Molecules*, 2021, 26, 7139. https://doi.org/10.3390/molecules26237139.

Tumor cells treated with BP-M345 undergo apoptotic cell death

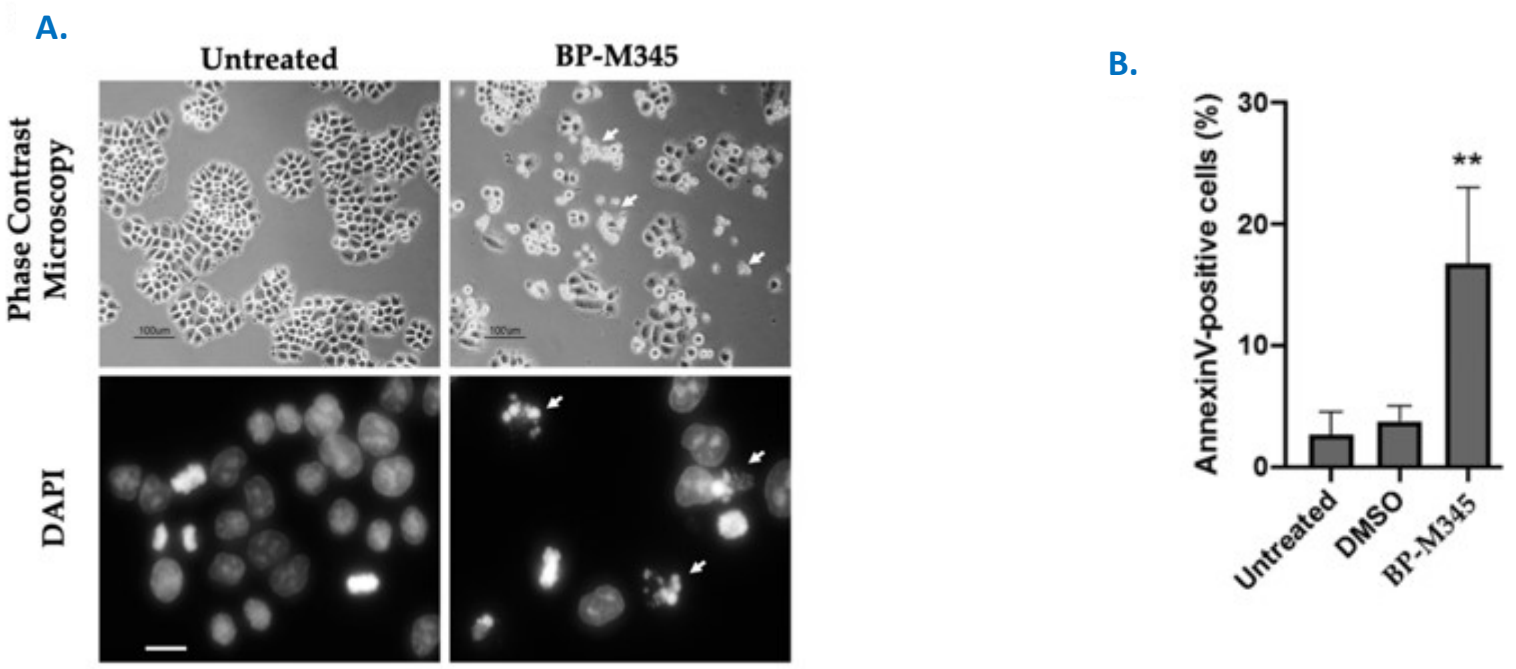

(A). Representative phase contrast microscopy (Top) and DAPI staining (Bottom) images of untreated cells and cells treated with 0.74 µM of BP-M345, after 24 hours exposure, showing accumulation of floating (arrows) and condensing cells (arrows), respectively, suggesting cell death. **(B).** Quantification of Annexin V-positive cells of the data shown in A with statistical relevance of ** $p < 0.01$ by unpaired t-test from three independent experiments.

Novais P. *et al.*, *Molecules*, 2021, 26, 7139. https://doi.org/10.3390/molecules26237139.

Identified as promising antiproliferative agents with some selectivity for tumor cells

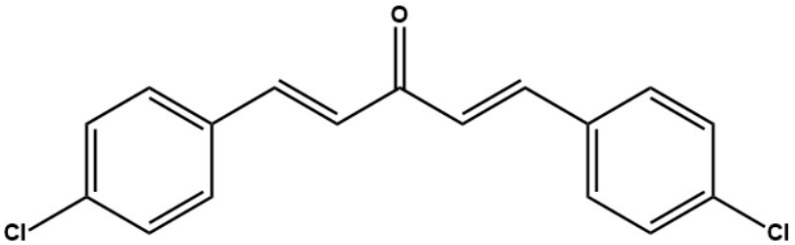

BP-C4
Dual Inhibitor of p53-MDM2/X interactions

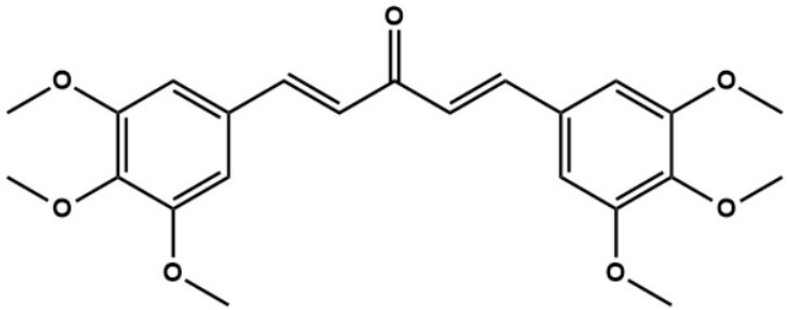

BP-M345
Antimitotic activity

Optimization:

- ✓ Potency
- ✓ Selectivity
- ✓ Structure-activity relationship studies

Research plan

GROUP A2:
substitution by a cyclic C5 bridge

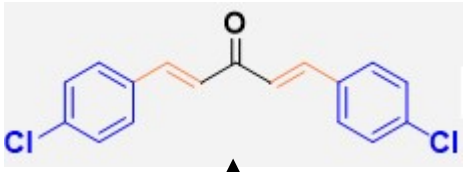

GROUP A1:
Bioisosteric substitution of A ring

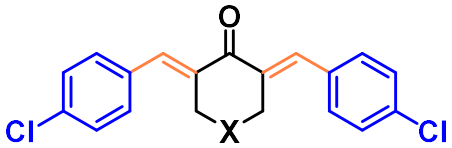

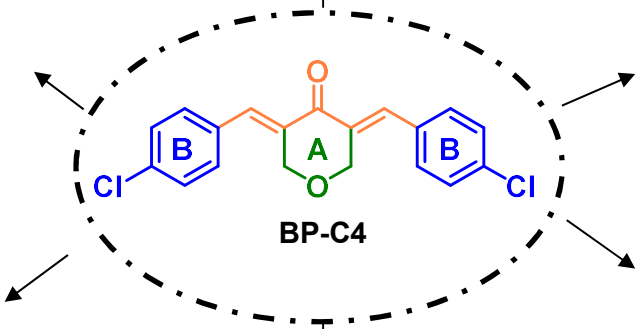

BP-C4

GROUP B1:
Selective reduction of dienone moiety

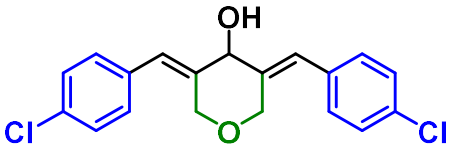

GROUP D:
α-conformationally restricted chalcone derivatives

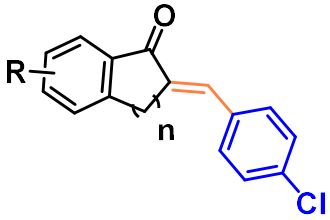

GROUP C:
Substitution by prenyloxy groups

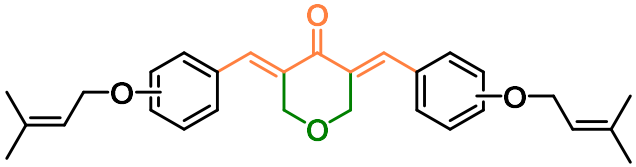

GROUP B2:
Selective reduction of dienone moiety

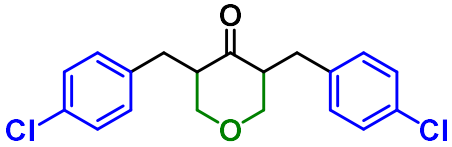

Moreira J. *et al.*, *Pharmaceuticals*, 2023, 16(10), 1354; https://doi.org/10.3390/ph16101354.

Group A

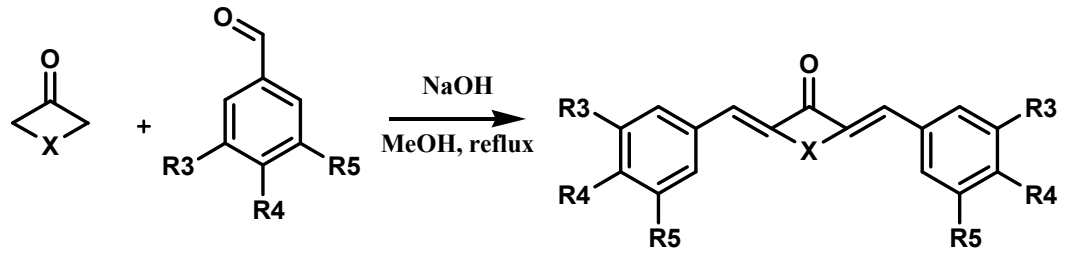

17: X=¢, R3=R5=H, R4=Cl
18: X=CH_2CH_2, R3=R5=H, R4=Cl
19: X=$CH_2CH_2CH_2$, R3=R5=H, R4=Cl
20: X=CH_2SCH_2, R3=R5=H, R4=Cl

η=31-90%

Group D

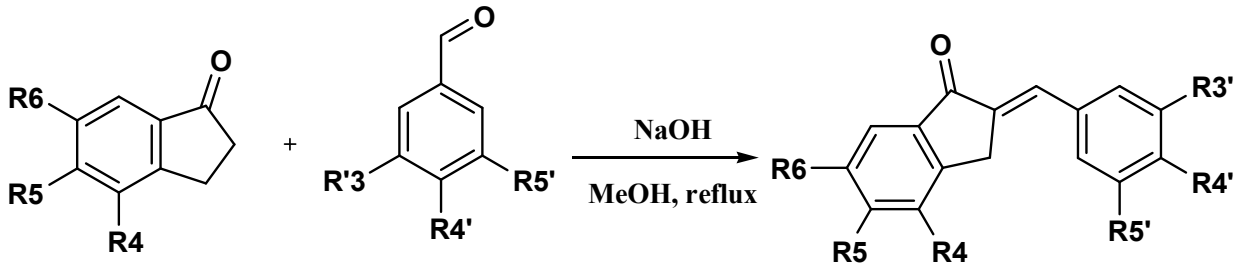

6: R4=R5=R6=R3'=R5'=H, R4'=Cl
7: R6=R3'=R5'=H, R4=R5=OCH_3, R4'=Cl
8: R4=R3'=R5'=H, R5=R6=OCH_3, R4'=Cl

η=47-86%

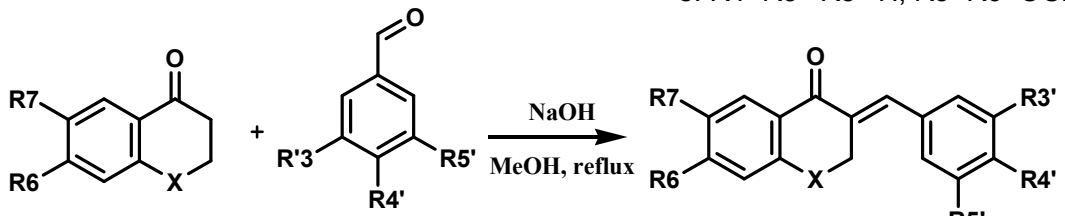

13: X=C, R6=R7=R3'=R5'=H, R4'=Cl
14: X=C, R3'=R5=H, R6=R7=OCH_3, R4'=Cl
15: X=O, R6=R7=R3'=R5'=H, R4'=Cl
16: X=S, R6=R7=R3'=R5'=H, R4'=Cl

η=23-90%

Moreira J. *et al*., *Pharmaceuticals*, **2023**, 16(10), 1354; https://doi.org/10.3390/ph16101354.

Group B

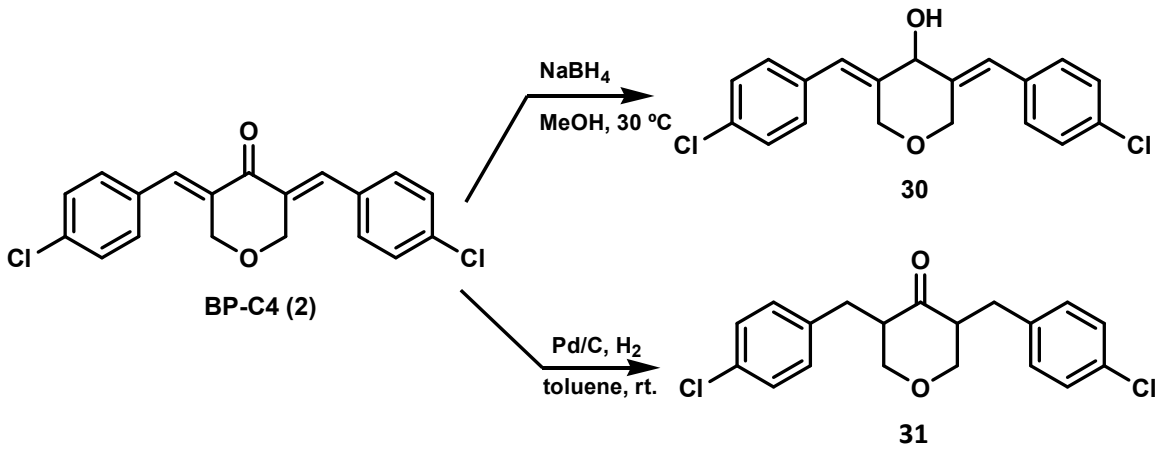

η=47-86%

Group C

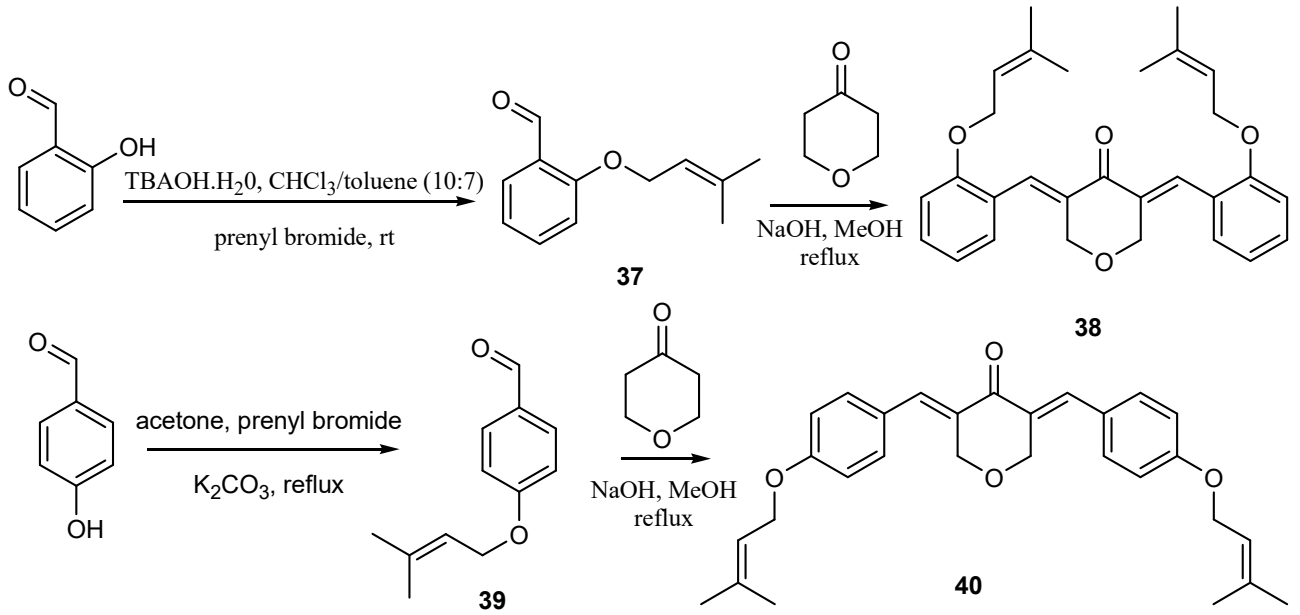

η=50%

η=25%

Moreira J. *et al*., *Pharmaceuticals*, 2023, 16(10), 1354; https://doi.org/10.3390/ph16101354.

✓ **Most of compounds displayed GI_{50} values < 10 µM**

Compound	GI_{50}			SI1	SI2
	HCT116 $p53^{+/+}$	HCT116 $p53^{-/-}$	HFF-1		
BP-C4	6.25 ± 1.18	10.13 ± 0.47	36.2 ± 5.54	1.62	5.79
CTC-C4 (16)	0.69 ± 0.07	7.95 ± 0.85	3.62 ± 0.99	11.5	5.25
BA-C4 (17)	2.18 ± 0.59	3.55 ± 0.05	27.10 ± 1.25	1.63	12.43

The results are expressed as mean ± standard deviation from three independent experiments. HCT116 $p53^{+/+}$: human colorectal tumor cell expressing p53; HCT116 $p53^{-/-}$: human colorectal tumor cell with deleted p53; HFF-1: fibroblasts, non-tumor cell line; SI1:Selective index 1 (GI_{50} of HCT116 $p53^{-/-}$/GI_{50} of HCT116 $p53^{+/+}$); SI2:Selective index 2 (GI_{50} of HFF-1/GI_{50} of HCT116 $p53^{+/+}$).

CTC-C4 (16) showed potent and seletive growth inhibitory effect on HCT116 cells over cells with deleted p53

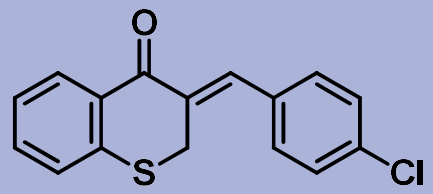

CTC-C4 (16)

BA-C4 (17) showed potent and seletive growth inhibitory effect on HCT116 cells when compared to HFF-1

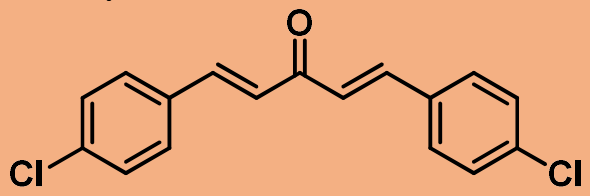

BA-C4 (17)

CTC-C4 (16):

- ✓ potential inhibitor of the p53-MDM2 interaction

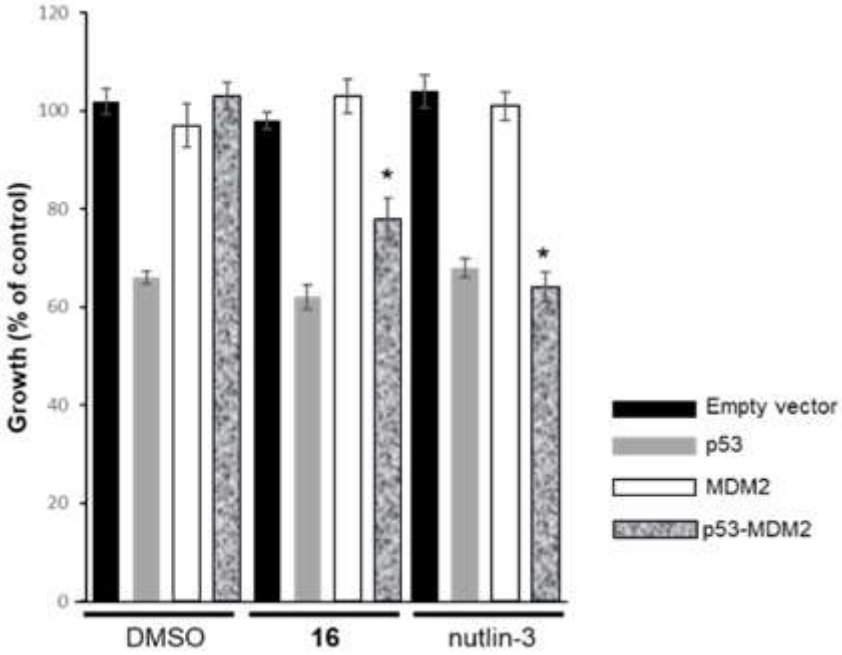

Data are mean ± SEM of four-five independent experiments; (*p < 0.05).

- ✓ BA-C4 (17):
- ✓ Induced apoptotic cell death (A)
- ✓ Cleaved PARP (B)
- ✓ Decreased anti-apoptotic protein BCL-2 (B)

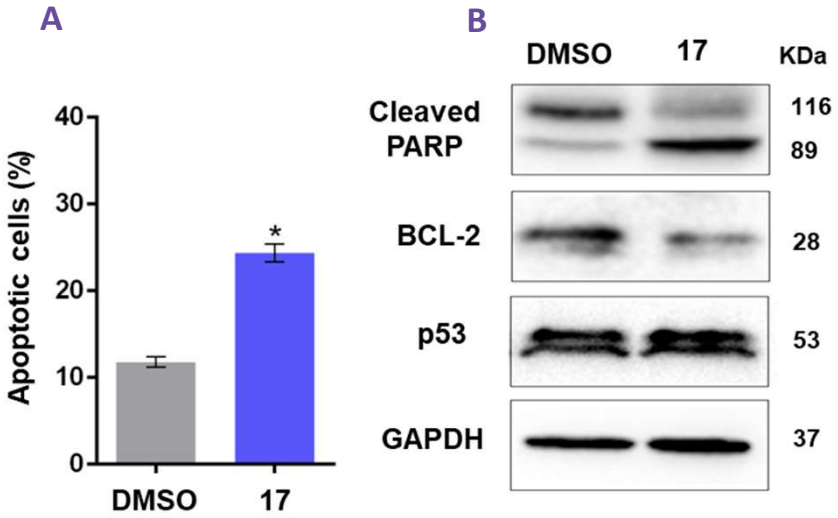

Data are mean ± SEM of three independent experiments (*p < 0.05, unpaired Student's t-test). Immunoblots are representative of three independent experiments. GAPDH was used as a loading control.

Moreira J. *et al*., *Pharmaceuticals*, 2023, 16(10), 1354; https://doi.org/10.3390/ph16101354.

Conclusions

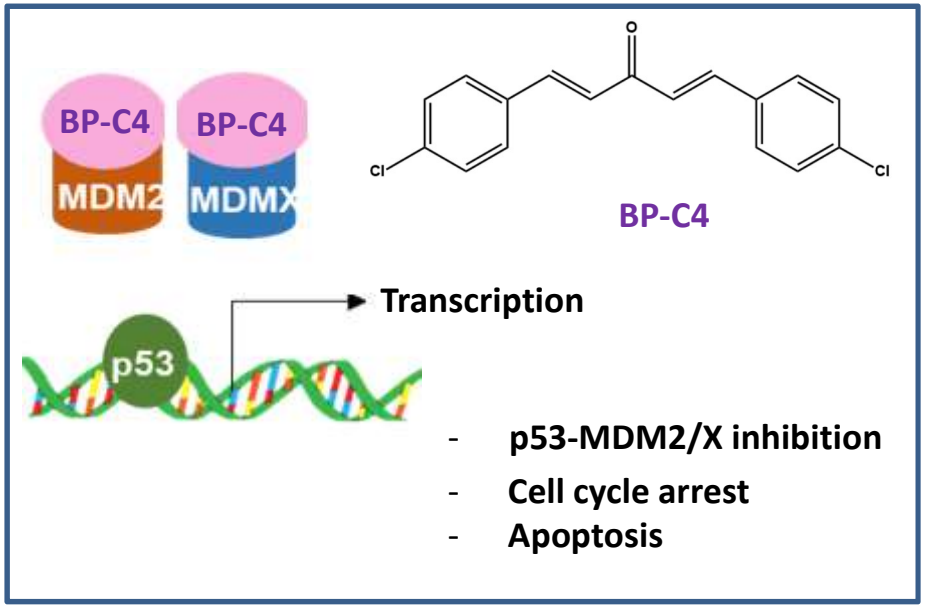

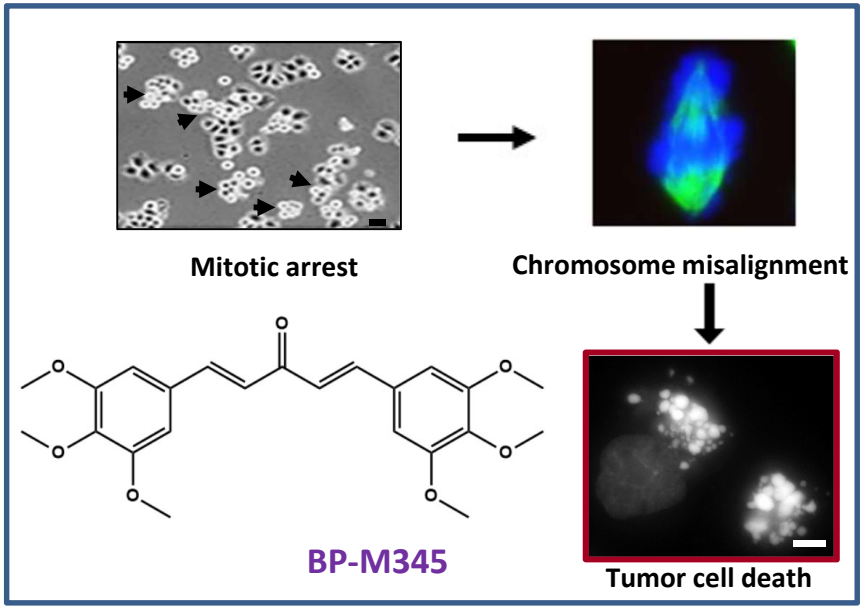

Molecular optimization

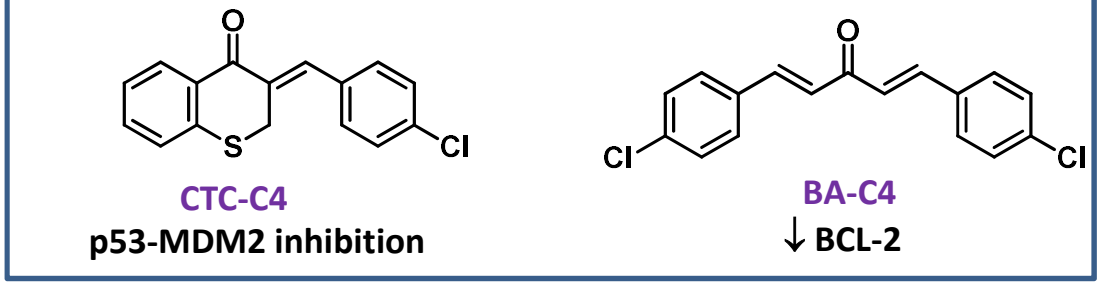

Acknowledgments

CIIMAR – Interdisciplinary Centre of Marine and Environmental Research
Marine Natural products and medicinal chemistry research group
Joana Moreira
Danilo Correia
Sara Cravo
Andreia Palmeira
Madalena Pinto

Joana Almeida
Joana Loureiro
Helena Ramos
Lucília Saraiva

Pedro Novais
Patricia Silva
Hassan Bousbaa

Isabel Amorim

This research was partially supported by the Strategic Funding UIDB/04423/2020 and UIDP/04423/2020 (Group of Marine Natural Products and Medicinal Chemistry - CIIMAR) and UIDB/50006/2020 (LAQV/REQUIMTE), through national funds provided by the FCT and ERDF, within the framework of the program PT2020 and by CESPU - Cooperativa de Ensino Superior Politécnico e Universitário under the project Flav4Tumor-GI2-CESPU-2022.